



**Universiteit
Leiden**
The Netherlands

Exploring ubiquitin and ISG15 biology with chemical tools

Gan, J.

Citation

Gan, J. (2022, June 7). *Exploring ubiquitin and ISG15 biology with chemical tools*. Retrieved from <https://hdl.handle.net/1887/3308336>

Version: Publisher's Version

License: [Licence agreement concerning inclusion of doctoral thesis in the Institutional Repository of the University of Leiden](#)

Downloaded from: <https://hdl.handle.net/1887/3308336>

Note: To cite this publication please use the final published version (if applicable).

Chapter 4.

Development of small molecule inhibitors targeting murine USP18

Jin Gan, Vito Pol, Hans van Dam, Raymond Kooij, Daniel J. Fernandez, Klaus-Peter Knobloch, Aysegul Sapmaz, Paul P. Geurink, Huib Ovaa

Manuscript in preparation

ABSTRACT

The ubiquitin-like modifier ISG15 plays a central role in modulating host signaling pathways to restrict microbial infection. USP18 is the major ISG15 deconjugating enzyme in both human and mouse cells and inhibition of USP18 activity is associated with enhanced viral resistance and tumor suppression. Here we identify the first generation of USP18 inhibitors by screening of an in-house covalent small-molecule library. The identified inhibitors were functional against both mouse and human USP18 *in vitro*, but more potent toward the murine enzyme. Experiments with intact cells proved that the USP18 inhibitors are cell-permeable and specific to murine USP18 over other human and mouse deubiquitinases. The two most potent inhibitors, PG157 BB7 and 2K04, also engage with endogenous mouse USP18 and increase cellular ISGylation in mouse EL4 cells after IFN- β stimulation.

INTRODUCTION

Interferon-stimulated gene 15 (*ISG15*) encodes a 17kDa ubiquitin-like modifier whose expression and conjugation is strongly upregulated by type I interferon (IFN) [1]. ISG15, expressed in a precursor form, is enzymatically processed into the mature form by cleavage of its C-terminus [2]. Free ISG15 can block NEDD4 ubiquitin ligase function [3] and stabilize USP18 in human cells [4]. Alternatively, it is secreted to the extracellular space as a cytokine to elicit IFN- γ secretion from lymphocytes [5] or peripheral blood mononuclear cells (PBMCs) [6]. Conjugation of ISG15 to substrate proteins (ISGylation) is mediated by a sequential cascade of E1, E2 and E3 enzymes [7, 8]. The ISGylation process can be reversed by deISGylase enzymes that remove ISG15 from the target proteins. The IFN-inducible protein USP18 represents the main cellular deISGylase [9], but also has enzyme-independent functions in inhibiting interferon signaling [10, 11].

ISGylation plays a critical role in antiviral response by modifying either viral or host proteins [12]. Genetic inactivation of USP18 enzymatic activity in cells or (USP18^{C61A/C61A} knock-in) mice leads to enhanced ISGylation upon IFN- β , poly(I:C), or LPS stimulation and elevated ISGylation is accompanied by increased viral resistance against vaccinia virus, influenza B virus, and coxsackievirus infections [13, 14]. Moreover, the level of ISG15 and ISGylation is found to be enhanced in many cancer cells; however, the role of ISGylation in anti-tumor or pro-tumor function in cell-based studies is controversial [15, 16]. A recent *in vivo* study using immunocompetent mice provided evidence for a tumor-suppressor function of the ISG15-ISGylation network in breast cancer. Polyomavirus mT-induced breast tumor growth was found to be enhanced in ISG15 E1 enzyme Ube11-deleted (KO) mice, and suppressed in USP18^{C61A/C61A} mice [17]. These studies indicate that USP18 is a promising target in antiviral and potential anti-tumor treatment.

In this study, we developed the first generation of USP18 inhibitors. Two of them, 2K04 and 2L12, were initially identified through a substrate assay based high-throughput screen using an in-house covalent small-molecule library. Further medicinal chemistry endeavor yielded the structurally related inhibitor PG157 BB7. All three inhibitors were functional against murine and human USP18 *in vitro*, but more potent toward murine USP18. Further study revealed that these USP18 inhibitors are cell-permeable, and selectively engage with murine USP18 without inhibiting the enzymatic activity of other deubiquitinases in cells. Moreover, the two most potent inhibitors PG157 BB7 and 2K04 increased cellular ISGylation in mouse EL4 cells after IFN- β stimulation.

RESULTS

High-throughput screening yielded potent and selective USP18 inhibitors

To identify USP18 inhibitors, we performed a high-throughput screen (HTS) using a previously developed in-house compound library. The library contains potential covalent cysteine-reactive small-molecule DUB inhibitors created by in-plate synthesis. The components to make the molecules were synthesized or purchased and the final coupling between the building blocks was achieved by dispensing small volumes (<1 μL) of the components along with coupling reagents into a 1536 well plate by acoustic dispensing using an Echo550. This way >22,000 unique compounds were prepared as crude reaction mixtures in 1536 well plates. LC-MS analysis was used to confirm compound formation and purity.

HTS was performed using a murine USP18 (mUSP18) biochemical activity assay that relies on cleavage of the quenched fluorogenic substrate murine ISG15 C-terminal domain linked Rhodamine (mISG15ct-Rhodamine), which releases the fluorescent dye Rhodamine110 upon USP18-mediated processing. As such, USP18 activity is reflected by an increase of fluorescent signal intensity. We also screened several DUBs (including 4 USP family DUBs structurally related to USP18) with the library, but instead using Ub-Rhodamine as substrate. This Ub-Rhodamine screen was done as a control to test the selectivity of the compounds. In the initial screen, 1.25 μM of each compound was incubated with mUSP18 (or related DUBs) for 30 min prior to addition of the substrate. A fluorescence intensity read-out was performed for 60 min and the percentage of inhibition was normalized to the controls: 0% inhibition for DMSO and 100% inhibition for 10 mM *N*-ethylmaleimide (NEM). From the initial list, two compounds showing >70% inhibition were of particular interest: 2K04 and 2L12. These structurally similar compounds displayed 95% and 75% inhibition of mUSP18, respectively, and did not inhibit any of the DUBs screened, which suggested a high degree of mUSP18 selectivity.

To further characterize the newly identified inhibitors, dose-response (DRP) studies were performed. We determined IC_{50} values of 0.18 μM and 0.48 μM for 2K04 and 2L12, respectively (Figure 1A). As these compounds were assayed in crude mixtures in the library, we re-synthesized, purified and characterized both compounds. Experiments with the purer-grade compounds confirmed the HTS results and showed the compounds to be about twice as potent with IC_{50} values of 0.095 μM and 0.24 μM for 2K04 and 2L12, respectively (Figure 1A, Table 1). These findings along with some of the other hits from this screen and some results from previous screens on mUSP18 led us to undertake a small medicinal chemistry endeavor. This resulted in the generation of an even more potent inhibitor structurally related to 2K04 and 2L12: PG157BB7, which has an IC_{50} of 0.035 μM (Figure 1B, Table 1). As control, we also synthesized the PG157BB7-stereoisomer PG157BB6, which has an inverted stereocenter. This compound is >300 times less potent towards mUSP18 (Figure 1B, Table 1).

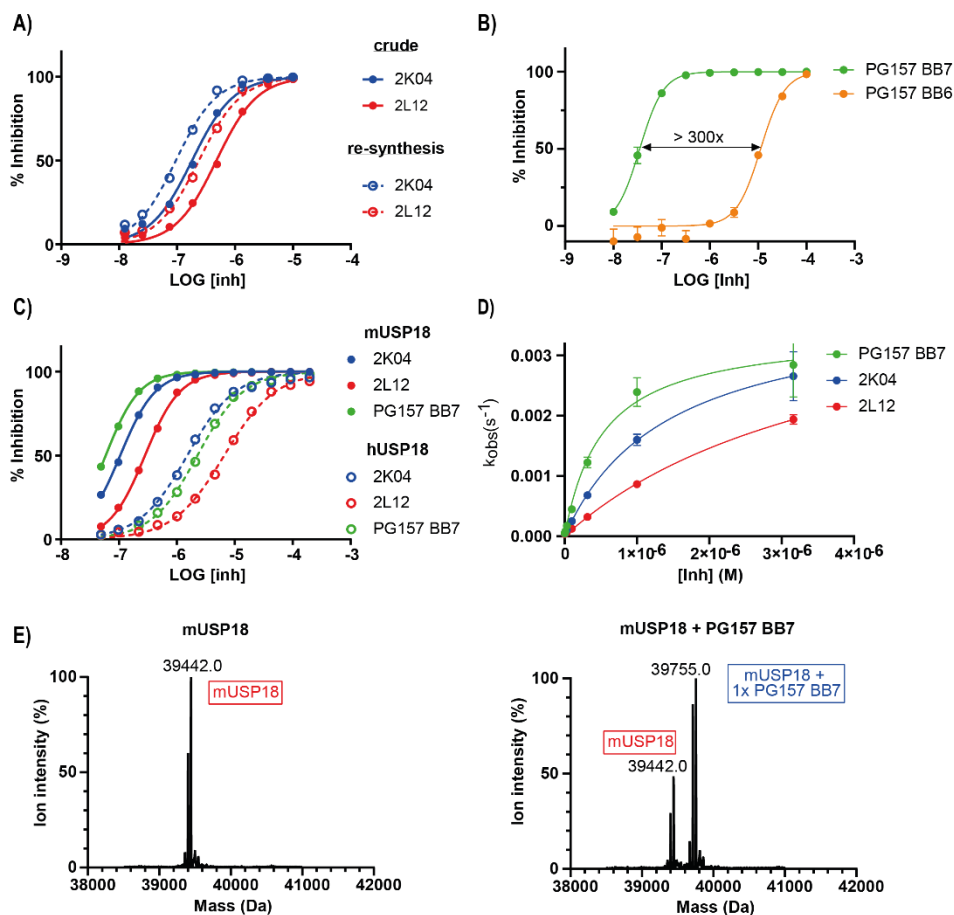


Figure 1. Inhibitory data of small-molecule covalent USP18 inhibitors. (A) Dose-response (DRP) curves of HTS hits after cherry-picking from the library plates (crude) and re-synthesis. (B) DRP curves of the most potent USP18 inhibitor and its stereoisomer (negative control compound). (C) DRP curves of three USP18 inhibitors towards murine and human USP18. (D) Curves used to determine the kinetics of covalent inhibition for the three mUSP18 inhibitors. (E) LC-MS analysis of covalent complex formation between mUSP18 and PG157BB7. MS trace of mUSP18 before (left) and after (right) treatment with PG157BB7.

We assessed the inhibitory potency of the compounds towards human USP18 (hUSP18) using hISG15ct-Rhodamine as substrate for the cleavage assays. All three compounds inhibited hUSP18 with micromolar affinity, but compared to mUSP18-inhibition a big difference in potency was observed (Figure 1C, Table 1). Based on their expected mode of action, i.e., covalent inhibitors targeting cysteine residues, we set out to determine more relevant biochemical parameters: the rate of inactivation (k_{inact}) and the inhibitory/binding constant (K_i) [18]. This was done by pre-incubating different concentrations of the inhibitors with the substrate prior to the addition of mUSP18. The observed first order rate constant (k_{obs}) revealed that

all three compounds have a similar inactivation rate but PG157BB7 displays the highest binding affinity (i.e. lowest K_I). This further demonstrates that PG157BB7 has the highest rate of covalent bond formation k_{inact}/K_I (Table 2).

IC50 (μ M)	mUSP18	hUSP18
2K04	0.095	1.5
2L12	0.24	6.6
PG157 BB7	0.035	2.3
PG157 BB6	11.3	n.d.

Table 1. IC50 values of the compounds against murine and human USP18.

	k_{inact} (s^{-1})	K_I (μ M)	k_{inact}/K_I ($M^{-1} s^{-1}$)
2K04	0.0040	1.54	2,597
2L12	0.0036	2.94	1,224
PG157 BB7	0.0034	0.52	6,538

Table 2. Covalent kinetic parameters for the mUSP18 inhibitors.

Next, we used LC-MS analysis to further confirm covalent complex formation between mUSP18 and PG157BB7. The MS trace of mUSP18 before and after treatment with PG157BB7 showed the formation of complex with a mass difference of 313 Da, the molecular mass of PG157BB7 (Figure 1E). Notably, we detected only one molecule of the inhibitor covalently bound to each mUSP18 molecule. Altogether, we identified three potent and selective small-molecule inhibitors of mUSP18, with PG157BB7 being the most potent one.

USP18 inhibitors are cell-permeable and inhibit murine USP18 in cells

We assessed the ability of PG157 BB7, 2K04 and 2L12 to inhibit mUSP18 in cells, via gel-based activity-based protein profiling (ABPP) [19, 20]. As a negative control we used PG157BB6, the stereoisomer of PG157BB7. In brief, HEK293T cells overexpressing Flag-tagged mUSP18 were incubated with increasing concentrations of the USP18 inhibitors. Following cell lysis, lysates were incubated with Rhodamine-tagged murine ISG15 C-terminal domain propargylamine (Rho-mISG15ct-PA) activity-based probe [21]. This probe covalently labels the active site cysteine of deISGlation enzymes that are not already blocked by inhibitors. The labeled enzymes are resolved by SDS-PAGE and imaged by in-gel fluorescence. All three inhibitors were engaged with cellular mUSP18 in a dose-dependent manner, indicating that these inhibitors can penetrate the cell membrane (Figure 2, Supplementary Figure 1A). The effective concentrations of the inhibitors corresponded with the IC50 values determined in vitro: PG157 BB7 and 2K04 displayed inhibition at 1μ M, while 2L12 was less potent, with an evident inhibition at 10

μM . (Figure 1, Table 1). With the negative control compound PG157 BB6 we only observed inhibition at 100 μM , the highest dose.

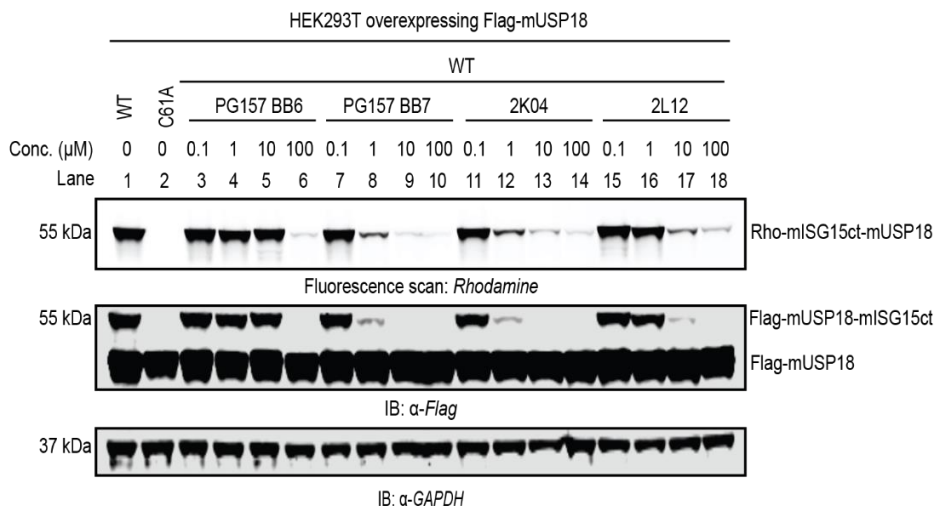


Figure 2. Inhibition of Flag-mUSP18 by the indicated compounds in HEK293T cells. Flag-mUSP18 (WT or catalytic dead mutant C61A) was transiently transfected in HEK293T cells. After 24 hours, cells were treated with indicated inhibitors at indicated concentrations for 4 hours. Cell lysates were incubated with Rho-mISG15ct-PA probe for 5 minutes, and subjected to SDS-PAGE, gel fluorescence scanning, and immunoblotting. Top: fluorescence scan of Rho-mISG15ct-PA probe labelled mUSP18 (see Supplementary figure 1A for full image scan). Middle: anti-Flag immunoblot data corresponding to probe labelled and unlabeled Flag-mUSP18. Bottom: anti-GAPDH immunoblot data validating equal loading of each sample.

PG157 BB7 and 2K04 are specific for USP18 and do not inhibit other DUBs

USP18 belongs to the USP DUB family according to phylogenetic analysis [22]. Therefore, we wondered whether the identified USP18 inhibitors can inhibit other USPs. To address this, we subjected the HEK 293T lysates from cells treated with the USP18 inhibitors to Rhodamine-tagged ubiquitin propargylamine (Rho-Ub-PA) activity-based probe [20] (Figure 3A). In this assay, we did not detect any band corresponding to USP18, corroborating with previous findings that USP18 is an ISG15-specific isopeptidase with no reactivity towards ubiquitin [9]. All inhibitors, including control PG157 BB6, did not display any detectable differences between the compound-treated cells and the DMSO control until 10 μM .

Since ISG15 and USP18 are strongly upregulated by type I interferon, we next assessed the selectivity of PG157 BB7 and 2K04 among murine DUBs in IFN- β -stimulated mouse EL4 cells. Gel-based activity based DUB profiling showed again, good selectivity until 10 μM for all compounds; the off-target inhibition of PG157 BB7 was even modest compared to 2K04 at 100 μM (Figure 3B).

Besides DUBs, there were also no observable off-targets within deISGylases, which were detected by the Rho-mISG15ct-PA probe in both HEK 293T and EL4 cells. (Supplementary Figure 1A, B).

To overcome the insufficient sensitivity of the fluorescence readout in gel-based probe profiling, we tested inhibition by 250 nM PG157 BB7 on a panel of recombinant human DUBs using *in vitro* ubiquitin-based fluorogenic substrate cleavage. In this assay PG157 BB7 did not inhibit any of the 42 DUBs except mUSP18, which was tested with mISG15ct-Rhodamine substrate (Figure 3C). Overall, our data indicate selectivity of the new inhibitors (especially PG157 BB7) for USP18 across all tested DUBs.

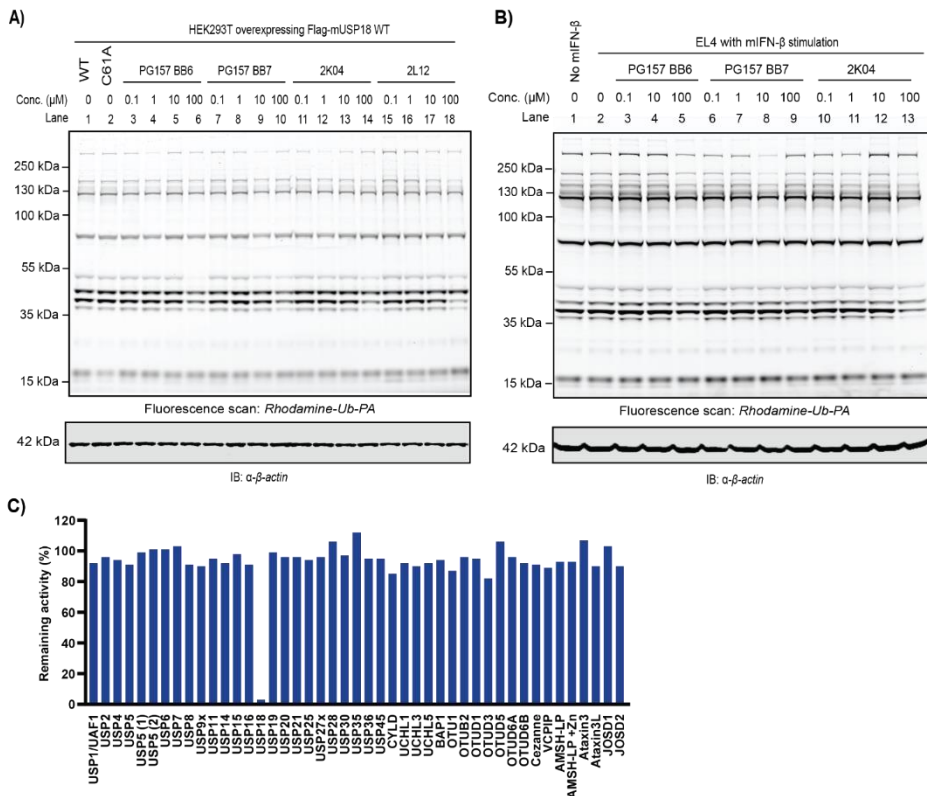


Figure 3. DUB off-target assessment of USP18 inhibitors. (A) Gel-based ABPP selectivity assessment using a Rho-Ub-PA probe in lysates of HEK293T cells overexpressing Flag-mUSP18. Top: fluorescence scan of Rho-Ub-PA probe labelled human DUBs. Bottom: anti-β-actin immunoblot data validating equal loading of each sample. (B) Gel-based ABPP selectivity assessment using the Rho-Ub-PA probe in mIFN-β stimulated mouse EL4 cell lysates. Top: fluorescence scan of Rho-Ub-PA probe labelled murine DUBs. Bottom: anti-β-actin immunoblot data validating equal loading of each sample. (C) Commercial human DUB specificity screen (one replicate) with 250 nM PG157 BB7.

USP18 inhibitor treatment results in endogenous USP18 inhibition and accumulated ISGylation in mouse EL4 cells

USP18 is the major deISGylase to remove ISG15 from target proteins and genetic inactivation of USP18 isopeptidase activity leads to enhanced ISGylation *in vivo* and in cells [23]. We therefore examined whether the USP18 inhibitors enhance cellular ISGylation. Accordingly, mouse EL4 cells were stimulated with IFN- β for 24 hours to induce cellular ISGylation, and then treated for 4 hours with increasing concentrations of USP18 inhibitors. The cell lysates were analysed by immunoblotting with an ISG15 antibody and Rho-mISG15ct-PA ABP probe assays. Treatments with PG157 BB7 and 2K04 significantly elevated cellular ISGylation in a dose dependent manner as maximum accumulation of ISGylation was reached at 10 μ M of either inhibitor. However, the stereoisomer control PG157 BB6 showed very limited effects even at 100 μ M (Figure 4A). Inhibition of the activity of endogenous USP18 was confirmed by anti-mUSP18 immunoblotting (Figure 4B). Interestingly, treatment with USP18 inhibitors greatly increased the IFN- β induced protein levels of mUSP18 (Figure 4B).

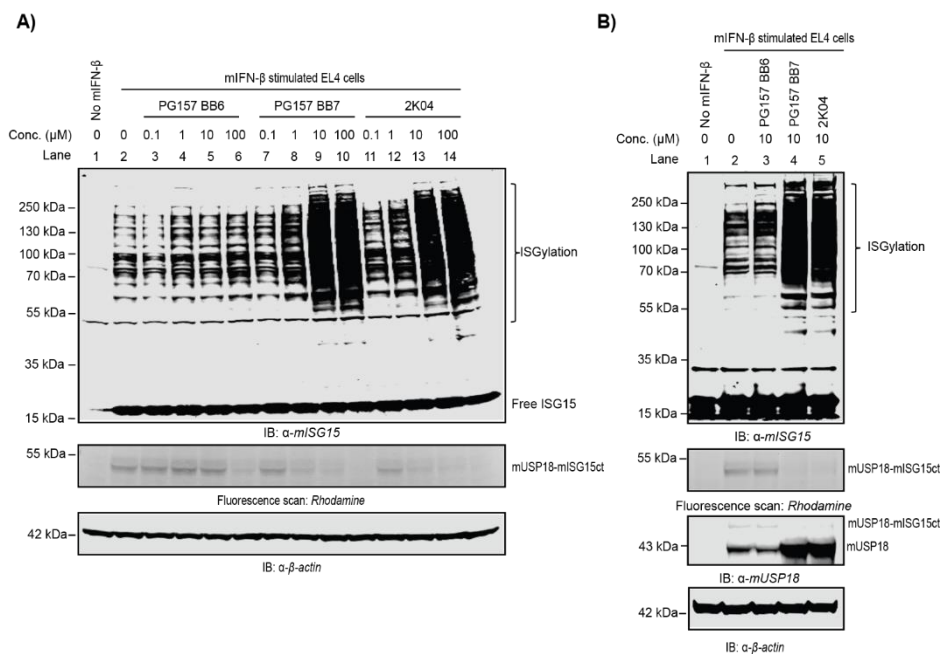


Figure 4. Accumulation of ISGylation and endogenous mUSP18 inhibition in mIFN- β stimulated mouse EL4 cells. (A) Cells were first stimulated with mouse IFN- β for 24 hours, then treated for 4 hours with the indicated inhibitor concentrations. Top: cell lysates were subjected to immunoblotting (anti-mISG15). Middle: Cell lysates were incubated with Rho-mISG15ct-PA for 5 minutes, then subjected to SDS-PAGE and gel fluorescence scanning (see Supplementary figure 1B for the full image scan). Bottom: anti- β -actin immunoblot data validating equal loading of each sample. (B) Cells were first stimulated with mouse IFN- β for 24 hours, then treated with 10 μ M of the indicated inhibitors for 4 hours. Top: cell lysates were subjected to immunoblotting (anti-mISG15). Middle: Cell lysates were incubated with Rho-mISG15ct-PA for 5 minutes, then subjected to SDS-

PAGE, gel fluorescence scanning and immunoblotting (anti-mUSP18). Bottom: anti- β -actin immunoblot data validating equal loading of each sample.

DISCUSSION

In the past decades, USP18's *in vivo* function [24-27], substrate specificity [9, 28], protein structure [21], and substrates [29, 30] have been widely studied, and many physiological studies related with USP18 highlighted the need of potent and select small-molecule inhibitors targeting USP18's isopeptidase function for either research or therapeutic purposes.

In this study, we developed three USP18 inhibitors (PG157 BB7, 2K04 and 2L12) with nanomolar to submicromolar affinity and we provided evidence that these inhibitors bind USP18 in a covalent manner. The inhibitors were validated by *in vitro* substrate cleavage assays, and (interference with) activity-based probe binding. It still remains elusive where the inhibitors act on USP18 at the molecular level. They might directly engage with the active-site cysteines (C61 in mouse USP18, C64 in human USP18), or bind allosterically to other amino acids or grooves to induce a steric hindrance effect. A cocrystal structure or proteomics data of USP18 bound with inhibitors is needed to explain the inhibitory mode in the future.

We showed very promising selectivity of the three USP18 inhibitors across both human and mouse DUBs with DUB profiling, but still need to confirm this with a proteome-wide selectivity study. IsoTOP-ABPP (isotopic Tandem Orthogonal Proteolysis – Activity-Based Protein Profiling) [31], MS-based thermal proteome profiling [32], or CITE-Id (Covalent Inhibitor Target-site Identification) [33] are possible techniques to investigate the selectivity of the identified compounds across the proteome.

Examination of the effects of the USP18 inhibitors in mouse EL4 cells showed accumulation of cellular ISGylation, which is line with previous USP18 genetic studies [26]. Independent of its ISG15 deconjugating activity, USP18 can also act as a negative regulator of type I and type III interferon signaling [10, 11]. As we don't know where the inhibitors bind to USP18, and whether inhibitor binding can induce a conformational change and/or affect USP18 protein-protein interaction, this ISGylated accumulation could, in theory, either result from enzymatic USP18 inhibition, or from disruption of USP18's non-enzymatic inhibition of IFN signaling. To minimize putative effects of non-enzymatic inhibition, we added the inhibitors 24 hours after the IFN- β stimulation, when interferon-induced protein expression reaches its steady state levels [27]. Moreover, we limited the treatment time to only 4 hours. Therefore, the observed enhanced accumulation of ISGylation is most likely caused by the inhibition of USP18's enzymatic function. However, we still need to check effects of the inhibitors on the non-enzymatic function of USP18 in future studies.

It should be noted here that only a very limited amount of mouse cell lines was found to show enhanced ISGylation upon USP18 inhibitor treatment, including EL4 (T lymphoblast), A20 (B lymphoblast, data not shown), and primary B cells isolated from mice (data not shown). This might be due to differences in IFN- β signaling strength and/or USP18 protein levels in the cells examined. Interestingly, the total levels of mUSP18 were strongly increased by 4h inhibitor treatment of EL4 cells. Therefore, the binding of the inhibitors to mUSP18 might result in interference with USP18 degradation. In fact, it was previously reported that binding of free ISG15 to USP18 results in reduced ubiquitination by E3 ligase complex SCF^{Skp2} and subsequently stabilization in human cells [4]. However,

mouse cells don't seem to have a similar system [34]. Anyhow, our inhibitors appear valuable tools to study the regulation of mouse USP18 expression and stability. Our inhibitors displayed inhibition of both murine and human USP18 *in vitro*, but we have only tested the effect on murine USP18 in cells so far. Since they are less potent against human USP18, it is still needed to optimize them for testing on human USP18 in cells.

Collectively, this study reports the development of small-molecule inhibitors of murine and human USP18 isopeptidase activity. Since, treatment of mouse EL4 cells leads to enhanced cellular ISGylation, these inhibitors can be a good starting point to test USP18-targeted therapeutic hypotheses in mouse models, and serve as a valuable research tool to further investigate USP18's function, regulation, and biochemical mechanisms.

ACKNOWLEDGMENTS

This work was supported by a VICI grant (no. 724.013.002) from The Netherlands Organization for Scientific Research (NWO) to H.O. Grant (no. ICI00026) from Institute for chemical immunology to A.S. J.G. was supported by the European Cooperation in Science and Technology (COST) with a short-term scientific mission grant (STSM, actin number: CA15138) to test mUSP18 inhibitors *in vivo*. Dr. Birol Cabukusta is acknowledged here for his insightful suggestions and critical reading.

1. Haas, A.L., et al., *Interferon induces a 15-kilodalton protein exhibiting marked homology to ubiquitin*. 1987. **262**(23): p. 11315-11323.
2. Potter, J.L., et al., *Precursor processing of pro-ISG15/UCRP, an interferon-beta-induced ubiquitin-like protein*. J Biol Chem, 1999. **274**(35): p. 25061-8.
3. Okumura, A., P.M. Pitha, and R.N. Harty, *ISG15 inhibits Ebola VP40 VLP budding in an L-domain-dependent manner by blocking Nedd4 ligase activity*. Proc Natl Acad Sci U S A, 2008. **105**(10): p. 3974-9.
4. Zhang, X., et al., *Human intracellular ISG15 prevents interferon-alpha/beta over-amplification and auto-inflammation*. Nature, 2015. **517**(7532): p. 89-93.
5. Recht, M., E.C. Borden, and E. Knight, Jr., *A human 15-kDa IFN-induced protein induces the secretion of IFN-gamma*. J Immunol, 1991. **147**(8): p. 2617-23.
6. Bogunovic, D., et al., *Mycobacterial disease and impaired IFN- γ immunity in humans with inherited ISG15 deficiency*. Science, 2012. **337**(6102): p. 1684-8.
7. Zhang, D. and D.E. Zhang, *Interferon-stimulated gene 15 and the protein ISGylation system*. J Interferon Cytokine Res, 2011. **31**(1): p. 119-30.
8. Villarroya-Beltri, C., S. Guerra, and F. Sanchez-Madrid, *ISGylation - a key to lock the cell gates for preventing the spread of threats*. J Cell Sci, 2017. **130**(18): p. 2961-2969.
9. Malakhov, M.P., et al., *UBP43 (USP18) specifically removes ISG15 from conjugated proteins*. J Biol Chem, 2002. **277**(12): p. 9976-81.
10. Arimoto, K.I., et al., *STAT2 is an essential adaptor in USP18-mediated suppression of type I interferon signaling*. Nat Struct Mol Biol, 2017. **24**(3): p. 279-289.
11. Malakhova, O.A., et al., *UBP43 is a novel regulator of interferon signaling independent of its ISG15 isopeptidase activity*. The EMBO journal, 2006. **25**(11): p. 2358-2367.
12. Perng, Y.C. and D.J. Lenschow, *ISG15 in antiviral immunity and beyond*. Nat Rev Microbiol, 2018. **16**(7): p. 423-439.
13. Ketscher, L., et al., *Selective inactivation of USP18 isopeptidase activity in vivo enhances ISG15 conjugation and viral resistance*. Proc Natl Acad Sci U S A, 2015. **112**(5): p. 1577-82.
14. Kespohl, M., et al., *Protein modification with ISG15 blocks coxsackievirus pathology by antiviral and metabolic reprogramming*. Sci Adv, 2020. **6**(11): p. eaay1109.
15. Han, H.G., H.W. Moon, and Y.J. Jeon, *ISG15 in cancer: Beyond ubiquitin-like protein*. Cancer Lett, 2018. **438**: p. 52-62.
16. Zuo, C., et al., *ISG15 in the tumorigenesis and treatment of cancer: An emerging role in malignancies of the digestive system*. Oncotarget, 2016. **7**(45): p. 74393-74409.

17. Fan, J.B., et al., *Type I Interferon Regulates a Coordinated Gene Network to Enhance Cytotoxic T Cell-Mediated Tumor Killing*. *Cancer Discov*, 2020. **10**(3): p. 382-393.
18. Strelow, J.M., *A Perspective on the Kinetics of Covalent and Irreversible Inhibition*. *SLAS Discov*, 2017. **22**(1): p. 3-20.
19. Resnick, E., et al., *Rapid Covalent-Probe Discovery by Electrophile-Fragment Screening*. *J Am Chem Soc*, 2019. **141**(22): p. 8951-8968.
20. Ekkebus, R., et al., *On terminal alkynes that can react with active-site cysteine nucleophiles in proteases*. *J Am Chem Soc*, 2013. **135**(8): p. 2867-70.
21. Basters, A., et al., *Structural basis of the specificity of USP18 toward ISG15*. *Nat Struct Mol Biol*, 2017. **24**(3): p. 270-278.
22. Clague, M.J., S. Urbé, and D. Komander, *Breaking the chains: deubiquitylating enzyme specificity begets function*. *Nature Reviews Molecular Cell Biology*, 2019. **20**(6): p. 338-352.
23. Swatek, K.N., et al., *Irreversible inactivation of ISG15 by a viral leader protease enables alternative infection detection strategies*. *Proceedings of the National Academy of Sciences*, 2018. **115**(10): p. 2371-2376.
24. Ritchie, K.J., et al., *Dysregulation of protein modification by ISG15 results in brain cell injury*. *Genes Dev*, 2002. **16**(17): p. 2207-12.
25. Rempel, L.A., et al., *Ubp43 gene expression is required for normal Isg15 expression and fetal development*. *Reprod Biol Endocrinol*, 2007. **5**: p. 13.
26. Ketscher, L., et al., *Selective inactivation of USP18 isopeptidase activity in vivo enhances ISG15 conjugation and viral resistance*. *Proceedings of the National Academy of Sciences*, 2015. **112**(5): p. 1577-1582.
27. Goldmann, T., et al., *USP18 lack in microglia causes destructive interferonopathy of the mouse brain*. *The EMBO Journal*, 2015. **34**(12): p. 1612-1629.
28. Basters, A., et al., *Molecular characterization of ubiquitin-specific protease 18 reveals substrate specificity for interferon-stimulated gene 15*. *FEBS J*, 2014. **281**(7): p. 1918-28.
29. Pinto-Fernandez, A., et al., *Deletion of the deISGylating enzyme USP18 enhances tumour cell antigenicity and radiosensitivity*. *Br J Cancer*, 2020.
30. Zhang, Y., et al., *The in vivo ISGylome links ISG15 to metabolic pathways and autophagy upon *Listeria monocytogenes* infection*. *Nat Commun*, 2019. **10**(1): p. 5383.
31. Senkane, K., et al., *The Proteome-Wide Potential for Reversible Covalency at Cysteine*. 2019. **58**(33): p. 11385-11389.
32. Franken, H., et al., *Thermal proteome profiling for unbiased identification of direct and indirect drug targets using multiplexed quantitative mass spectrometry*. *Nat Protoc*, 2015. **10**(10): p. 1567-93.

33. Browne, C.M., et al., *A Chemoproteomic Strategy for Direct and Proteome-Wide Covalent Inhibitor Target-Site Identification*. Journal of the American Chemical Society, 2019. **141**(1): p. 191-203.
34. Jiménez Fernández, D., S. Hess, and K.-P. Knobeloch, *Strategies to Target ISG15 and USP18 Toward Therapeutic Applications*. Frontiers in Chemistry, 2020. **7**.

Supporting information

MATERIALS AND METHODS

IC₅₀ Determination

The assays were performed in “nonbinding surface flat bottom low flange” black 384-well plates (Corning) at room temperature in a buffer containing 50 mM Tris·HCl, 100 mM NaCl, pH 7.6, 2.0 mM cysteine, 1 mg/mL 3-[(3-cholamidopropyl)-dimethylammonio]propanesulfonic acid (CHAPS), and 0.5 mg/mL γ -globulins from bovine blood (BGG). Each well had a final volume of 20.4 μ L. The compounds were dissolved in 10 mM DMSO stocks, and appropriate volumes were transferred to the empty plates using a Labcyte Echo acoustic dispenser. A DMSO back-fill was performed to obtain equal volumes of DMSO (400 μ L) in each well. *N*-ethylmaleimide (NEM, 10 mM) was used as a positive control (100% inhibition) and DMSO as a negative control (0% inhibition). A 10 μ L portion of buffer was added, and the plate was vigorously shaken for 20s. Next, 5 μ L of recombinant mUSP18 (46-368 aa) [1] or hUSP18 (16-372 aa) [2] was added to a final concentration of 25 nM followed by incubation for 120 min. A 5 μ L portion of the substrate (mISG15ct-RhoMP for mUSP18, hISG15ct-RhoMP for hUSP18) was added (final concentration 400 nM), and the increase in fluorescence over time was recorded using a BMG Labtech PHERAstar plate reader (excitation 487 nm, emission 535 nm). The initial enzyme velocities were calculated from the slopes, normalized to the positive and negative controls, and plotted against the inhibitor concentrations (in M) using the built-in equation “[inhibitor] vs response – variable slope (four parameters), least-squares fit” with constraints “Bottom = 0” and “Top = 100” in GraphPad Prism 7 software to obtain the IC₅₀ values.

In case of the k_{inact}/K_I determinations the order of mUSP18 and substrate addition was reversed and no incubation time was used. All data fitting and calculations were done using GraphPad Prism 7 software. The fluorescence intensities were plotted against time (in seconds) after a baseline correction using the DMSO control for each inhibitor concentration. The data were fitted to the equation $FI = (v_i/k_{\text{obs}})[1 - e^{-k(\text{obs})t}]$.

Covalent Complex Formation Mass Spectrometry Analysis

Samples of 1.4 μ M mUSP18 in 70 μ L buffer containing 50 mM Tris·HCl, 100 mM NaCl at pH 7.6 and 2.0 mM cysteine were prepared. These samples were treated with 1 μ L of DMSO or 1 μ L of a 10 mM PG157BB7 stock solution in DMSO (140 μ M final concentration) and incubated for 30 min at room temperature. Samples were then diluted 3-fold with water and analyzed by mass spectrometry by injecting 1 μ L into a Waters XEVO-G2 XS Q-TOF mass spectrometer equipped with an electrospray ion source in positive mode (capillary voltage 1.2 kV, desolvation gas flow 900 L/h, T = 60 °C) with a resolution of R = 26 000. Samples were run using two mobile phases: (A) 0.1% formic acid in water and (B) 0.1% formic acid in CH₃CN on a Waters Acquity UPLC protein BEH C4 column [300 Å, 1.7 μ m (2.1 \times 50 mm²), flow rate = 0.5 mL/min, run time = 14.00 min, column T = 60 °C, and mass detection 200–2500 Da]. Gradient: 2–100% B. Data processing was performed using Waters MassLynx mass spectrometry software 4.1, and ion peaks were deconvoluted using the built-in MaxEnt1 function.

Cell lines and reagents

Human HEK293T (Cat# ATCC® CRL-3216™) and mouse EL4 (Cat# ATCC® TIB-39™) cells were cultured under standard conditions in Dulbecco's modified Eagle's medium (DMEM) (Gibco) supplemented with 8% FCS (Biowest) and 1% penicillin/streptomycin at 37 °C and 5% CO₂. All cell lines were tested for mycoplasma contamination using MycoAlert™ Mycoplasma Detection Kit (Lonza, Catalog #: LT07-318) on a monthly basis.

Interferon β from mouse (mIFN- β) was purchased from Sigma-Aldrich (Cat# I9032).

Murine USP18 overexpression and in-cell inhibition assays

For DNA transfections, HEK293T cells were seeded into 6-well plate to achieve 50–60% confluence the following day and then transfected with plasmids Flag-mUSP18 wildtype (Flag-mUSP18 wt) and Flag-mUSP18 catalytic cysteine-to-alanine mutant (Flag-mUSP18 C61A) [2] using PEI (polyethylenimine, Polysciences Inc., Cat# 23966) as follows: 200 μ L DMEM medium without supplements was mixed with DNA and PEI (1 mg/mL) with a ratio at 1:3 (eg: 1 μ g DNA : 3 μ L PEI), incubated at RT for 20 min, and added drop-wise to the cells. At 24 hours following transfection, cells were incubated with indicated compounds at the indicated final concentrations at 37 °C for 4 hours, then washed twice with PBS and harvested for further analysis.

Generation of ISGylation and in-cell inhibition assay

Mouse EL4 cells were stimulated with 300 U/mL mouse IFN- β to induce ISGylation and USP18 expression. At 24 hours following stimulation, cells were incubated with indicated compounds at the indicated final concentrations at 37 °C for 4 hours, then washed twice with PBS and harvested for further analysis.

mISG15ct-based activity-based probe (Rhodamine-mISG15ct-PA) labeling

The in-cell inhibition of mUSP18 was assessed by using DUB probe labelling assay [3]. In brief, cell pellets were resuspended in HR buffer (50 mM Tris-HCl, 5 mM MgCl₂, 250 mM sucrose, 2 mM TCEP and a Protease inhibitor tablet (Roche), pH 7.4), and lysed by sonication (Bioruptor, Diagenode, high intensity for 10 minutes with an ON/OFF cycle of 30 seconds) at 4°C. 40 μ g clarified cell lysate was labelled with Rhodamine-mISG15ct-propargylamide probe (final concentration at 1 μ M) at 37 °C for 30 min. Reactions were stopped by the addition of LDS (lithium dodecyl sulfate) sample buffer (Invitrogen Life Technologies, Carlsbad, CA, USA) containing 2.5% β -mercaptoethanol, followed by boiling for 7 minutes.

SDS-PAGE, in-gel fluorescence scanning, and immunoblotting

Samples were resolved on precast Bis-Tris NuPAGE Gels (Invitrogen, including 4-12%, and 10% for different samples) using MOPS buffer (Invitrogen Life Technologies, Carlsbad, CA, USA).

For fluorescence scan, labeled enzymes were visualized by in-gel fluorescence using a Typhoon FLA 9500 imaging system (GE Healthcare Life Sciences) (Rhodamine channel for probe, Cy5 channel for protein marker).

For immunoblotting, proteins were transferred to a nitrocellulose membrane (Protran BA85, 0.45 μ m, GE Healthcare) at 300 mA for 3 hours. The membranes were blocked in 5% milk (skim milk powder, LP0031, Oxiod) in 1 \times PBS (P1379, Sigma-Aldrich), incubated with a primary antibody diluted in 5% milk in 0.1% PBS-Tween 20 (PBST) for overnight at cold room, washed three times for 5 min in 0.1% PBST, incubated with the

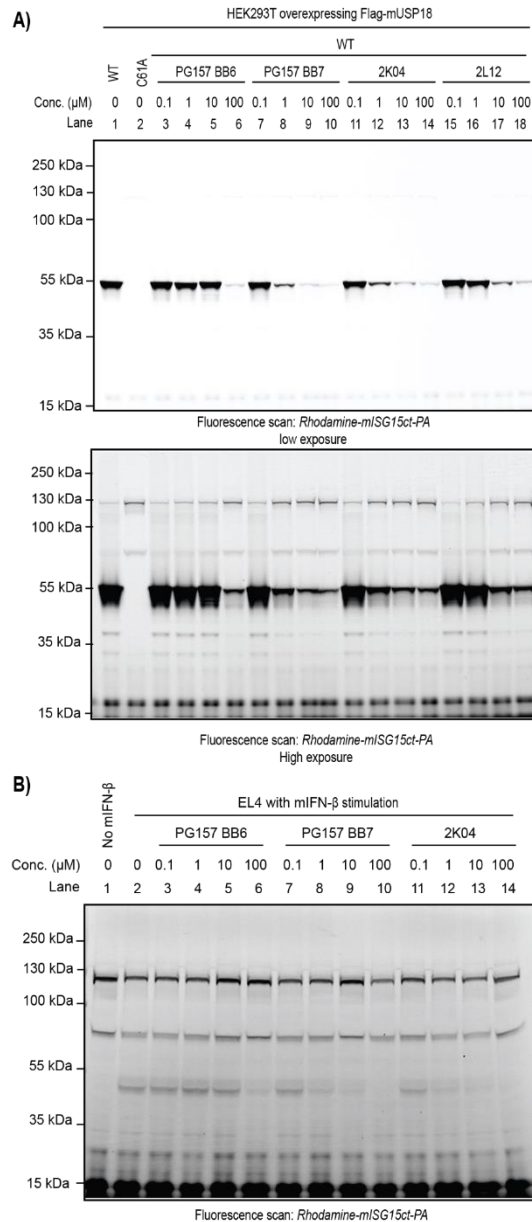
secondary antibody diluted in 5% milk in 0.1% PBST for 1 hour, and washed three times again in 0.1% PBST. The signal was visualized using a LICOR Odyssey system.

The following primary antibodies were used: mouse anti-Flag (M2, Sigma-Aldrich), rabbit anti-mISG15 [4], rabbit anti-mUSP18 [5], mouse anti-GAPDH (1D4, Enzo Lifesciences) or mouse anti- β -actin (clone AC-15, Sigma-Aldrich).

The following fluorescent secondary antibodies (from LICOR) were used: anti-mouse-680, anti-rabbit-800.

REFERENCES

1. Basters, A., et al., *Molecular characterization of ubiquitin-specific protease 18 reveals substrate specificity for interferon-stimulated gene 15*. FEBS J, 2014. **281**(7): p. 1918-28.
2. Basters, A., et al., *Structural basis of the specificity of USP18 toward ISG15*. Nat Struct Mol Biol, 2017. **24**(3): p. 270-278.
3. Resnick, E., et al., *Rapid covalent-probe discovery by electrophile-fragment screening*. 2019. **141**(22): p. 8951-8968.
4. Osiak, A., et al., *ISG15, an interferon-stimulated ubiquitin-like protein, is not essential for STAT1 signaling and responses against vesicular stomatitis and lymphocytic choriomeningitis virus*. Mol Cell Biol, 2005. **25**(15): p. 6338-45.
5. Ketscher, L., et al., *Selective inactivation of USP18 isopeptidase activity in vivo enhances ISG15 conjugation and viral resistance*. Proceedings of the National Academy of Sciences, 2015. **112**(5): p. 1577-1582.



Supplementary Figure 1. Full image scan of Rho-mISG15ct-PA probe labelled enzymes in cell lysates. (A) Gel-based ABPP assessment using a Rho-mISG15ct-PA probe in HEK293 cell lysates overexpressing Flag-mUSP18, corresponding to top band in Figure 2. Top: fluorescence scan in low exposure; Bottom: fluorescence scan in high exposure. (B) Gel-based ABPP assessment using a Rho-mISG15ct-PA probe in mIFN- β stimulated mouse EL4 cell lysates, corresponding to middle band in Figure 4A.

